Studies of 2,5;6,10;8,10-Tri-μ-hydro-nonahydro-*nido*-nonaborate(1−), [B₉H₁₂]⁻: Preparation, Crystal and Molecular Structure,† Nuclear Magnetic Resonance Spectra, Electrochemistry, and Reactions

Grant B. Jacobsen, Dominic G. Meina, John H. Morris,* and Colin Thomson
Department of Pure and Applied Chemistry, University of Strathclyde, 295 Cathedral Street, Glasgow G1 1XL
Steven J. Andrews, David Reed, and Alan J. Welch
Department of Chemistry, University of Edinburgh, West Mains Road, Edinburgh EH9 3JJ
Donald F. Gaines
Department of Chemistry, University of Wisconsin, 1101 University Avenue, Madison, Wisconsin 53706, U.S.A.

Studies of 2,5;6,10;8,10-tri-μ-hydro-nonahydro-*nido*-nonaborate(1−) [B₉H₁₂]⁻ have involved new syntheses, which have led to crystals suitable for the determination of the X-ray crystal and molecular structure, through reactions of B₉H₁₃(SMe₂) with [OCN]⁻ or other bases. Crystallographic study of [N(PPh₃)₂][B₉H₁₂] reveals the structure of the anion to be that of a *nido*-nine-vertex cage, based on the parent bicapped square antiprism with one 5-connected vertex removed. The pentagonal open face is symmetrically bridged by three (μ-H) atoms (two involving the lowest connected boron), conferring effective C_s symmetry upon the polyhedron. Crystals are monoclinic, space group $P2_1/n$, with $a = 26.759(10)$, $b = 10.340(4)$, $c = 27.044(5)$ Å, $\beta = 103.47(2)°$, and $Z = 8$. Using 6 777 diffracted intensities recorded at 185 K on an Enraf-Nonius CAD4 diffractometer, the structure has been refined to R 0.0847, R' 0.1216. The ¹¹B, two-dimensional ¹¹B(COSY), and ¹H n.m.r. parameters all confirm the structural assignment and the n.m.r. spectra have been assigned unambiguously. Cyclic and a.c. voltammetry and coulometry of [B₉H₁₂]⁻ in several solvents at Pt led to the electrochemical parameters and to an isomer-specific electrochemical synthesis of *anti*-[B₁₈H₂₁]⁻. Chemically, the [N(PPh₃)₂]⁺ salt of [B₉H₁₂]⁻ reacted with HCl to give [B₉H₁₃Cl]⁻, whereas the [NBuⁿ₄]⁺ salt yielded *anti*-B₁₈H₂₂; reactions with CF₃CO₂H gave primarily *anti*-[B₁₈H₂₁]⁻

The [B₉H₁₂]⁻ anion has been known for many years and was originally isolated through degradative reactions of *nido*-decaborane(14),[1] and through treatment of B₉H₁₃L (L = SMe₂ or SEt₂) with strong base.[2] Over the last twenty years, there have been a number of attempts to establish the structure of the *nido*-[B₉H₁₂]⁻ anion. X-Ray diffraction studies[3] of the [NMe₄]⁺ and [NMe₂Et₂]⁺ salts were inconclusive because of disorder but did suggest that the ion was monomeric. The isoelectronic *nido*-carbaborane C₂B₇H₁₁ and its C-dimethyl derivative have been prepared[4] and the latter characterised by a single-crystal structure determination.[5] Although the observed architecture for this compound was found to be that expected (a bicapped square antiprism with a 5-connected vertex removed), the parent carbaborane did not yield crystals that were suitable for crystallographic study. However, ¹¹B and ¹H n.m.r. experiments suggested that the molecule has very low symmetry, existing as an enantiomorphic pair.[6]

Todd and co-workers[7,8] have suggested (from ¹¹B n.m.r. data) that the gross arrangement of boron atoms in [B₉H₁₂]⁻ is similar to that found in *arachno*-B₉H₁₃(MeCN),[9] although the data were not sufficiently definitive for the unambiguous determination of the structure. Although it may appear to be misleading to draw structural analogies between *nido*- and *arachno*-clusters with the *same* number of polyhedral atoms, this particular comparison does have some merit in that a 9-

debor-(1441) polyhedron is related to a 1,3-didebor-(12442) polyhedron by the formal breaking of only one connectivity.

Thus, it has long been assumed[10a] that [B₉H₁₂]⁻ has the boron skeleton of its *closo* parent, [B₁₀H₁₀]²⁻,[11] from which a high-connectivity vertex is removed.

We now report new syntheses of salts of the [B₉H₁₂]⁻ anion, from which crystals of [N(PPh₃)₂][B₉H₁₂] have proved suitable for X-ray crystallographic analysis. The crystallographic studies unambiguously identify the arrangement in the solid state, at least for the [N(PPh₃)₂]⁺ salt, as the *nido* derivative from the parent *closo*-[B₁₀H₁₀]²⁻, and give the locations of three non-terminal (bridging) cage hydrogen atoms.

We also report the complete assignment of the ¹¹B n.m.r. spectrum, established using the two-dimensional (COSY) technique, and the ¹H and ¹H-{¹¹B, c.w.} (c.w. = continuous wave) spectra‡ together with a correlation of the proton chemical shifts with the boron positions, which are entirely consistent with the solid-state structure.

In addition, the electrochemical properties of the anion have not been previously reported and we now present electrochemical studies of [B₉H₁₂]⁻ at Pt in the solvents acetonitrile, dichloromethane, pyridine, 1,3-dioxolane, 1,2-dichloroethane, tetramethylurea, and tetrahydrofuran. We report the isomer-specific electrochemical synthesis of *anti*-[B₁₈H₂₁]⁻. Electrochemical studies of [B₉H₁₂]⁻ at other anodes have led to an evaluation of the anodic dissolution technique for the preparation of metalloboranes.

[B₉H₁₂]⁻ had previously been shown to react with HCl in

---

‡ During the course of this work, a manuscript of a publication containing some ¹H n.m.r. data on the compound was received from Professor N. N. Greenwood.[12]

ethers (OR_2) to give $B_9H_{13}(OR_2)$[13] or in diethyl sulphide to give $B_9H_{13}(SEt_2)$.[8] We now report the addition reaction of HCl with $[N(PPh_3)_2][B_9H_{12}]$ in CH_2Cl_2 to give *arachno*-$[B_9H_{13}Cl]^-$. $[B_9H_{14}]^-$ was also shown to react with HCl and produced *anti*-$B_{18}H_{22}$ via initial hydrogen elimination to form the reactive B_9H_{13} intermediate.[13b] We have now found that reaction of $[NBu^n_4][B_9H_{12}]$ with HCl in CH_2Cl_2 produces *anti*-$B_{18}H_{22}$ presumably by addition of H^+ to form B_9H_{13}. Reaction of $[NBu^n_4][B_9H_{12}]$ with CF_3CO_2H in CH_2Cl_2 leads to $B_{10}H_{14}$ and *anti*-$[B_{18}H_{21}]^-$.

The $[B_9H_{12}]^-$ anion had previously been shown to react with mercury halides to give $B_{18}H_{22}$, $[B_9H_{10}Cl_2]^-$, $[B_9H_{11}Cl]^-$, and $[B_9H_{10}Br_2]^-$.[14]

Experimental

Reagents.—Decaborane(14) was purchased from the Callery Chemical Company and sublimed before use. $B_9H_{13}(SMe_2)$ was prepared from $B_{10}H_{14}$ via degradation of $B_{10}H_{12}(SMe_2)_2$ with MeOH.[2] $[N(PPh_3)_2][OCN]$ was obtained by treating $[N(PPh_3)_2]Cl$ with an equimolar quantity of Na[OCN] in water and extracting the product by phase transfer to CH_2Cl_2. The product was recrystallised from CH_2Cl_2–Et_2O to give white needle-like crystals. Other solvents and reagents were dried by standard procedures.

Synthesis of $[NBu^n_4][B_9H_{12}]$.—$[NBu^n_4][B_9H_{12}]$ was prepared by the literature method;[1,2] $[NMe_4][B_9H_{12}]$ was similarly obtained.

Synthesis of $[N(PPh_3)_2][B_9H_{12}]$.—$B_9H_{13}(SMe_2)$ (0.43 g, 2.5 mmol) and $[N(PPh_3)_2][OCN]$ (1.51 g, 2.6 mmol) were placed in a 250-cm^3 three-necked round-bottomed flask fitted with a reflux condenser under dry nitrogen. Dry 1,2-dichloroethane (*ca.* 25 cm^3) was introduced, the mixture was refluxed for 1.5 h, after which time a small quantity of a white precipitate, shown to be $B(OH)_3$, formed and the solution was filtered. Thin-layer chromatography of the filtrate on silica gel using CH_2Cl_2 as eluant showed a single major fraction $(R_f = 0.32)$. The solvent was removed under reduced pressure and the white solid was redissolved in the minimum quantity of CH_2Cl_2 and purified by chromatography on silica gel, using CH_2Cl_2 as eluant. The major fraction was collected, the solvent was removed under reduced pressure, and the white crystalline solid was recrystallised from CH_2Cl_2–n-pentane to yield crystallographic-quality colourless, needle-like crystals (yield 0.486 g, 30%) (Found: C, 66.6; H, 6.5; N, 2.2. Calc. for $C_{36}H_{42}B_9NP_2$: C, 66.7; H, 6.5; N, 2.2%).

Alternatively, an excess of $[N(PPh_3)_2][OCN]$ was added dropwise to a stirred solution of $B_9H_{13}(SMe_2)$ (0.69 g, 4.0 mmol) in hot ethanol. A crystalline white precipitate was formed which was filtered off and recrystallised from CH_2Cl_2–Et_2O. The colourless needles (1.9 g, 75%) were identical to those from other preparations.

Reactions of $B_9H_{13}(SMe_2)$ *with* $LiN=C(NMe_2)_2$.—A fresh solution of $LiN=C(NMe_2)_2$ (2 mmol) was prepared by treating a cooled solution of $HN=C(NMe_2)_2$ (0.25 cm^3, 2 mmol) in hexane (5 cm^3) and 1,2-dimethoxyethane (5 cm^3) with 1.7 mol dm^{-3} n-butyl-lithium (1.17 cm^3, 2 mmol) in a Schlenk tube under nitrogen.[15] The solution was warmed to room temperature and to it was added $B_9H_{13}(SMe_2)$ (0.35 g, 2 mmol) followed by 1,2-dimethoxyethane (2 cm^3) and the mixture stirred for 24 h. The solvents were removed under reduced pressure to yield a yellow oil. Thin-layer chromatography on silica (dichloromethane eluant) indicated three components, of which one was starting material. The two products had $R_f = 0.08$, 0.66. The mixture, separated by chromatography on silica using dichloro-

Table 1. 115.5-MHz [11]B and 360-MHz ^{1}H correlated[a] n.m.r. data for $B_9H_{13}[HN=C(NMe_2)_2]$ in CD_3CN

Boron position	$\delta(^{11}B)/$ p.p.m.[b]	$J(B-H)/$ Hz	$\delta(^{1}H)/$ p.p.m.[c]	Relative intensity	Proton assignment
7	11.45	148	3.57	1	Terminal
1	1.19	130	2.67	1	Terminal
4	−11.89	—	—		
6,8	−13.73	136	2.09	2	Terminal
5,9	−17.84	139	1.31	2	Terminal
2,3	−37.03	143	0.25	2	Terminal
			2.96	12	CH_3–N
			6.18	1	N–H
			−1.21	5	Bridge

[a] [11]B and ^{1}H data correlated from specific frequency decoupling experiments. [b] Reference $BF_3 \cdot OEt_2$. [c] Reference $SiMe_4$.

methane as eluant, gave a light orange solid and a yellow solid, identified by [11]B and [1]H n.m.r. spectroscopy as $B_9H_{13}[HN=C(NMe_2)_2]$ (0.29 g, 64%) and $[(Me_2N)_2C=NH_2][B_9H_{12}]$ (0.052 g, 11.5%), respectively (see Table 1).

When the reaction was carried out at 50 °C, the major product was $B_9H_{13}[HN=C(NMe_2)_2]$ $(R_f = 0.66)$, with minor products at $R_f = 0.45$, 0.25, and 0.1.

Reactions of $B_9H_{13}(SMe_2)$ *with Lithium Dibenzylamide.*—$LiN(CH_2Ph)_2$ (0.41 g, 2 mmol), which had been freshly prepared from dibenzylamine (0.38 g, 2.0 mmol) and a solution of n-butyl-lithium (2 mmol) in dry hexane (5 cm^3) and dry 1,2-dimethoxyethane (5 cm^3), was treated with $B_9H_{13}(SMe_2)$ (0.34 g, 2.0 mmol) in a Schlenk tube under nitrogen.[16] The reaction mixture was stirred for 24 h at room temperature, solvents were removed under vacuum, and the crude yellow oil was separated by chromatography on silica, using a mixture of MeCN–CH_2Cl_2 (1:9) as eluant. The main component yields a yellow oil, whose [11]B n.m.r. spectrum indicated $[B_9H_{12}]^-$. In separate experiments, the reaction mixture was heated to 40 °C for 2 h and the products again separated by chromatography. The [11]B n.m.r. spectra of the products again indicated $[B_9H_{12}]^-$, together with $B_9H_{13}L$, $B_8H_{12}L$, and BH_3L [$L = NH(CH_2-Ph)_2$].

Synthesis of $[N(PPh_3)_2][B_9H_{13}Cl]$.—A 100-$cm^3$ round-bottomed flask fitted with a stopcock adapter and magnetic stirrer was charged with $[N(PPh_3)_2][B_9H_{12}]$ (0.53 g, 0.82 mmol) and evacuated. Degassed CH_2Cl_2 was condensed in under vacuum, and the mixture warmed to room temperature until all the $[B_9H_{12}]^-$ salt had dissolved. The solution was cooled to −196 °C, gaseous HCl (0.30 g, 0.83 mmol) condensed in, and the mixture warmed to room temperature. After stirring for 3 h, the solvent was removed and the white solid was monitored as a single product $(R_f = 0.47)$ by thin-layer chromatography on silica, using CH_2Cl_2 as eluant. The product, purified by chromatography on silica and recrystallised from CH_2Cl_2–n-hexane, formed as colourless crystals (yield 0.2 g, 34%).

Molecular Structure Determination of $[N(PPh_3)_2][B_9H_{12}]$ (1).—A single crystal, *ca.* 0.1 × 0.05 × 0.05 cm, was mounted on a glass fibre using low-temperature adhesive. Preliminary Weissenberg photographs (Cu-K_α X-radiation) yielded space group and approximate cell dimensions. Although the presence of two independent ion pairs was thereby revealed, we felt that the ultimate goal merited the major crystallographic commit-

ment this entailed. However, it would clearly be beneficial to perform a low-temperature study in order to maximise the chances of locating the borane-H atoms and, therefore, the same crystal was transferred to an Enraf-Nonius CAD4 diffractometer and cooled slowly to ca. 185 K in a stream of cold nitrogen.

After an initial cell had been generated by the automatic centring of 25 low-angle reflections $(7 < \theta < 9°$, Mo-K_α X-radiation, $\bar{\lambda} = 0.710\,69$ Å), an asymmetric fraction of intensity data in the range $12 < \theta < 12.5°$ was rapidly recorded, from which 25 strong reflections were chosen and centred. The final cell dimensions and orientation matrix were generated by a least-squares fit.

Crystal data. $C_{36}H_{42}B_9NP_2$, $M = 648.0$, space group $P2_1/n$ (no. 14), $a = 26.759(10)$, $b = 10.340(4)$, $c = 27.044(5)$ Å, $\beta = 103.47(2)°$, $U = 7\,277.0$ Å^3, $Z = 8$, μ(Mo-K_α) = 1.42 cm^{-1}, $D_c = 1.183$, $D_m = 1.15$ g cm^{-3}, $F(000) = 2\,720$.

Collection and reduction of data. Three-dimensional intensity data $(+h, +k, \pm l)$ were recorded using a θ–2θ scan in 96 steps, in the range $1.0 < \theta < 23.0°$. Scan widths were given by A + $B\tan\theta$, where $A = 0.80$ and $B = 0.35$. After a rapid prescan, only those reflections considered sufficiently intense $[I \geqslant 0.5\sigma$-$(I)]$ were remeasured such that the final intensity had $I \geqslant 33\sigma(I)$ subject to a maximum scan period of 90 s. Two standard reflections were remeasured once every 3 600s of X-ray exposure time, but subsequent analysis of their net counts as functions of time showed no crystal decomposition or movement, or source variance over the data collection period (ca. 264 h). Data were corrected for Lorentz and polarisation effects but not for X-ray absorption. Of 11 378 independent reflections measured, 6 777 had $F_o \geqslant 5.0\sigma(F_o)$ and these were used for structure solution and refinement.

Solution and refinement of the structure. Subjection of the data to the MULTAN 80[17] direct-methods program yielded both P–N–P skeletons. Subsequent iterative refinement and difference electron-density syntheses yielded all the remaining non-hydrogen atoms. Structure factors were then weighted according to $w^{-1} = \sigma^2(F_o) + 0.001\,89(F_o{}^2)$. Phenyl groups were treated as rigid planar hexagons $\{C–C = 1.395, C–H = 1.08$ Å; $U_H = 0.05$ Å^2, the form of the isotropic thermal motion is given by $\exp[-8\pi^2 U(\sin^2\theta)/\lambda^2]\}$ with variable and individual isotropic thermal parameters for the carbons. With all the phosphorus, nitrogen, and boron atoms allowed anisotropic thermal vibrations, further refinement revealed all the remaining hydrogen atoms. These were assigned fixed isotropic thermal parameters $(U_H = 0.05$ Å$^2)$ but were allowed independent positional refinement. The 433 variables (including overall scale factor) were optimised by full-matrix least-squares refinement (data:variable ratio better than 15:1) which converged at $R = 0.0847$ and $R' = 0.1216$, where $R = \Sigma\|F_o| - |F_c\||/\Sigma|F_o|$ and $R' = \Sigma w(|F_o| - |F_c|)^2/\Sigma w|F_o|^2$. The maximum residue on the final difference map was 0.93 e Å^{-3}.

Structure refinement was carried out using the SHELX 76 system,[18] implemented on the Edinburgh Regional Computer Centre ICL2972 machine. Molecular-geometry calculations were made with XANADU[19] and XRAY 76[20] and figures constructed using ORTEP-II.[21]

N.M.R. Spectra.—Spectra were obtained at 250 MHz (^{1}H) and 80.2 MHz (^{11}B) on a Bruker WH 250 spectrometer and at 360 MHz (^{1}H) and 115.5 MHz (^{11}B) on a Bruker WH 360 spectrometer. In all cases, lock was achieved on the deuterium resonance of the deuteriated solvent. ^{1}H-$\{^{11}$B, broad band$\}$ and ^{1}H-$\{^{11}$B, c.w.$\}$ spectra were recorded and the proton shift data abstracted by difference from off-resonance decoupled spectra. Two-dimensional ^{11}B–^{11}B (COSY) spectra were obtained using the pulse sequence $D1$–$90°$–t_1–$90°$–acquire, where $D1$ is a relaxation delay (0.1 s), giving an overall acquisition time of

Table 2. ^{11}B, ^{1}H-$\{^{11}$B, c.w.$\}$ correlated,[a] and ^{11}B (COSY) n.m.r. spectra of anti-$[B_{18}H_{21}]^-$

$\delta(^{11}B)/$ p.p.m.[b]	Relative intensity	COSY coupling[c]	$\delta(^1H)/$ p.p.m.[d]	Relative intensity
11.5 (s)	1			
14.06	1	A B D	3.53	1
10.19	1		3.76	1
5.72	1	E	3.00	1
4.04	1		3.56	1
0.87 (s)	1	G		
−0.37	1	H	2.97	1
−3.73	2	D F	2.97	1
			2.67	1
−7.12	1	C	2.57	1
−9.89	2		2.14	1
			2.48	1
−12.70	2		2.66	1
			1.88	1
−23.33	1	E	−0.40	1
−28.46	1	B F G	−0.89	1
−38.44	1	A	0.20	1
−40.39	1	C H	0.21	1
			−1.04[e]	
			−0.160[e]	
			−1.93[e]	
			−3.34[e]	
			−3.94[e]	

[a] ^{11}B and ^{1}H data correlated from specific frequency decoupling experiments. [b] Reference BF$_3$·OEt$_2$; all resonances are doublets except those labelled (s) (*i.e.* singlet). [c] Borons which give rise to off-diagonal maxima are identified by a common letter. [d] Reference SiMe$_4$. [e] Bridges.

0.14 s. The data gave a 256 × 256 matrix, which was symmetrised prior to plotting.

Electrochemical Techniques.—Cyclic and a.c. voltammograms were obtained using instrumentation which has been described previously.[22] Coulometric and controlled potential synthesis was carried out using a Hi-Tek Instruments DT2101 Potentiostat and DVM-Voltage Integrator. The cell for synthetic work comprised two compartments separated by a Nafion 415 cation-exchange membrane. The anode was a Pt mesh and its potential was measured with reference to Ag wire in contact with CH$_2$Cl$_2$ containing [N(PPh$_3$)$_2$]Cl (0.1 mol dm^{-3}). It was separated from the anode solution by a porous ceramic sinter (Kent Industrial Measurements E.I.L. Analytical Instruments).

Electrochemical Synthesis of anti-$[B_{18}H_{21}]^-$.—The anode compartment of the preparative electrochemical cell was charged with [NBu$^n_4$][B$_9$H$_{12}$] (0.351 g, 1 mmol) dissolved in CH$_2$Cl$_2$ (20 cm^3) containing [NBu$^n_4$][BF$_4$] (0.1 mol dm^{-3}). The cathode compartment was charged with 20 cm^3 of aqueous HBF$_4$ (40% mol dm^{-3}). The potential of the anode was maintained at 1.5 V (with respect to the reference electrode). The current, initially *ca.* 40 mA, dropped to 2 mA after 2 h, when a total of 80 C had passed, corresponding to 83% of the theoretical for one-electron oxidation. The yellow anode solution was removed from the cell and the solvent distilled off under vacuum. The solid, redissolved in CH$_2$Cl$_2$, was chromatographed on silica, using CH$_2$Cl$_2$ as eluant. The first component eluted was identified as a trace of B$_{10}$H$_{14}$ by its ^{11}B n.m.r. spectrum. The second major component was identified by its ^{11}B, ^{11}B-$\{^1$H$\}$, and ^{1}H-$\{^{11}$B, c.w.$\}$ spectra (Table 2) as anti-$[B_{18}H_{21}]^-$ by comparison with the spectra of an authentic sample.[8,23]

Table 3. Fractional co-ordinates of refined atoms for (1) with estimated standard deviations in parentheses*

Atom	x	y	z	Atom	x	y	z
P(1)	0.220 24(6)	0.132 11(15)	0.177 16(6)	C(412)	−0.036 14(12)	0.609 2(3)	0.434 24(13)
P(2)	0.169 27(6)	−0.012 01(15)	0.082 65(6)	C(413)	−0.035 96	0.6752	0.479 28
N(1)	0.199 84(20)	0.019 3(5)	0.137 81(21)	C(414)	−0.076 81	0.7564	0.482 19
C(112)	0.141 45(13)	0.082 4(3)	0.223 72(12)	C(415)	−0.117 84	0.7716	0.440 06
C(113)	0.118 64	0.071 3	0.264 96	C(416)	−0.118 02	0.7056	0.395 02
C(114)	0.147 71	0.0926	0.314 23	C(411)	−0.077 17	0.6244	0.392 11
C(115)	0.199 58	0.1251	0.322 26	C(422)	0.004 02(14)	0.383 5(3)	0.327 26(13)
C(116)	0.222 40	0.1362	0.281 02	C(423)	0.033 63	0.2718	0.339 15
C(111)	0.193 33	0.1148	0.231 75	C(424)	0.021 53	0.1813	0.372 81
C(122)	0.310 75(13)	−0.002 5(3)	0.202 20(12)	C(425)	−0.020 18	0.2025	0.394 58
C(123)	0.363 61	−0.0171	0.220 83	C(426)	−0.049 80	0.3141	0.382 69
C(124)	0.394 31	0.0909	0.237 00	C(421)	−0.037 70	0.4046	0.349 03
C(125)	0.372 14	0.2135	0.234 54	C(432)	−0.064 45(12)	0.648 7(3)	0.243 34(13)
C(126)	0.319 27	0.2282	0.215 91	C(433)	−0.043 59	0.7351	0.213 98
C(121)	0.288 57	0.1201	0.199 74	C(434)	−0.007 00	0.8254	0.237 53
C(132)	0.228 35(12)	0.336 5(3)	0.114 15(13)	C(435)	0.008 74	0.8293	0.290 44
C(133)	0.212 74	0.4540	0.090 10	C(436)	−0.012 12	0.7430	0.319 81
C(134)	0.174 18	0.5262	0.104 05	C(431)	−0.048 71	0.6526	0.296 26
C(135)	0.151 22	0.4809	0.142 05	B(1)	0.370 8(4)	0.457 6(7)	0.050 2(4)
C(136)	0.166 82	0.3635	0.166 10	B(2)	0.419 9(4)	0.394 6(8)	0.057 5(4)
C(131)	0.205 39	0.2913	0.152 15	B(3)	0.363 9(4)	0.320 7(8)	0.081 6(4)
C(212)	0.260 26(13)	−0.120 9(3)	0.071 08(12)	B(4)	0.322 4(4)	0.362 3(8)	0.022 9(4)
C(213)	0.289 81	−0.2042	0.048 92	B(5)	0.373 9(4)	0.391 2(8)	−0.005 2(4)
C(214)	0.266 01	−0.2861	0.009 46	B(6)	0.396 3(4)	0.177 2(9)	0.070 2(4)
C(215)	0.212 66	−0.2848	−0.007 85	B(7)	0.329 3(4)	0.193 8(8)	0.041 5(4)
C(216)	0.183 11	−0.2015	0.014 31	B(8)	0.330 5(5)	0.245 6(9)	−0.022 0(4)
C(211)	0.206 91	−0.1196	0.053 77	B(10)	0.363 7(5)	0.106 6(8)	0.010 7(5)
C(222)	0.068 86(13)	−0.091 4(3)	0.041 89(12)	B(1′)	0.422 0(7)	0.076 8(12)	0.627 7(6)
C(223)	0.024 00	−0.1591	0.042 81	B(2′)	0.433 3(5)	0.166 8(10)	0.580 2(5)
C(224)	0.020 92	−0.2311	0.085 64	B(3′)	0.411 5(4)	0.243 3(11)	0.629 4(5)
C(225)	0.062 70	−0.2353	0.127 54	B(4′)	0.457 4(5)	0.161 8(10)	0.676 5(4)
C(226)	0.107 56	−0.1675	0.126 62	B(5′)	0.481 6(5)	0.075 2(9)	0.633 0(5)
C(221)	0.110 64	−0.0956	0.083 79	B(6′)	0.445 1(5)	0.340 2(11)	0.598 9(5)
C(232)	0.113 39(14)	0.207 1(4)	0.047 34(13)	B(7′)	0.463 9(5)	0.327 8(9)	0.664 9(4)
C(233)	0.100 21	0.3141	0.015 53	B(8′)	0.515 8(4)	0.209 4(11)	0.667 8(5)
C(234)	0.125 68	0.3371	−0.023 15	B(10′)	0.508 4(4)	0.357 3(10)	0.636 2(5)
C(235)	0.164 31	0.2531	−0.030 01	H(1)	0.371 3(14)	0.550 1(16)	0.058 3(14)
C(236)	0.177 49	0.1462	0.001 80	H(2)	0.464 2(14)	0.375 3(16)	0.071 8(14)
C(231)	0.152 03	0.1232	0.040 47	H(3)	0.357 3(14)	0.313 0(16)	0.123 2(14)
P(3)	−0.176 68(6)	0.411 61(16)	0.283 65(6)	H(4)	0.280 8(14)	0.413 0(16)	0.011 7(14)
P(4)	−0.077 82(6)	0.544 93(15)	0.333 36(6)	H(5)	0.388 6(14)	0.449 1(16)	−0.038 6(14)
N(2)	−0.134 46(20)	0.517 4(5)	0.304 02(20)	H(6)	0.418 0(14)	0.110 7(16)	0.108 9(14)
C(312)	−0.218 22(12)	0.473 6(3)	0.364 69(13)	H(7)	0.297 4(14)	0.127 2(16)	0.059 4(14)
C(313)	−0.257 95	0.4901	0.389 60	H(8)	0.299 9(14)	0.227 9(16)	−0.055 7(14)
C(314)	−0.308 64	0.4657	0.363 98	H(10)	0.360 5(14)	0.003 9(16)	0.005 1(14)
C(315)	−0.319 60	0.4248	0.313 44	H(25)	0.410 5(14)	0.326 7(16)	0.010 1(14)
C(316)	−0.279 88	0.4084	0.288 52	H(610)	0.406 4(14)	0.139 6(16)	0.019 5(14)
C(311)	−0.229 19	0.4327	0.314 15	H(810)	0.372 3(14)	0.161 8(16)	−0.024 4(14)
C(322)	−0.221 54(13)	0.330 7(3)	0.184 71(13)	H(1′)	0.377 7(14)	−0.035 9(16)	0.625 4(14)
C(323)	−0.240 42	0.3521	0.132 77	H(2′)	0.428 6(14)	0.134 7(16)	0.542 6(14)
C(324)	−0.238 95	0.4760	0.112 74	H(3′)	0.376 4(14)	0.280 2(16)	0.624 9(14)
C(325)	−0.218 60	0.5785	0.144 63	H(4′)	0.451 0(14)	0.146 2(16)	0.716 4(14)
C(326)	−0.199 72	0.5572	0.196 57	H(5′)	0.508 2(14)	−0.040 4(16)	0.641 4(14)
C(321)	−0.201 19	0.4333	0.216 60	H(6′)	0.423 3(14)	0.420 2(16)	0.577 0(14)
C(332)	−0.117 72(12)	0.204 4(3)	0.268 68(12)	H(7′)	0.468 4(14)	0.370 5(16)	0.690 8(14)
C(333)	−0.095 42	0.0828	0.279 99	H(8′)	0.547 1(14)	0.189 4(16)	0.688 0(14)
C(334)	−0.109 29	0.0058	0.317 01	H(10′)	0.538 0(14)	0.406 3(16)	0.644 0(14)
C(335)	−0.145 46	0.0505	0.342 71	H(25′)	0.494 3(14)	0.153 5(16)	0.595 7(14)
C(336)	−0.167 76	0.1721	0.331 40	H(610′)	0.486 6(14)	0.338 5(16)	0.583 0(14)
C(331)	−0.153 89	0.2491	0.294 38	H(810′)	0.527 2(14)	0.245 9(16)	0.628 6(14)

* The carbon atoms of the phenyl groups each have the same e.s.d. as that of the first quoted, C(ij2).

Electrochemical Oxidation of [B₉H₁₂]⁻ *in* MeCN.—In a typical experiment, the anode compartment of the preparative electrochemical cell was charged with [NBuⁿ₄][B₉H₁₂] (0.352 g, 1.0 mmol) dissolved in MeCN (20 cm³). The cathode compartment contained 20 cm³ of a solution of [NBuⁿ₄][BF₄] in MeCN (0.1 mol dm⁻³). The current, initially 40 mA, fell to 2 mA over a period of 1 h when the anode potential was maintained at 0.86 V, consuming a total of 94.5 C, corresponding to 98% of the theoretical for one electron per mol. The solvent was removed from the clear anolyte solution under reduced pressure, and the solid examined by t.l.c. on silica using CH₂Cl₂ as eluant. Two components (R_f 0.9 and 0.7) were

Table 4. Internuclear distances (Å) for (1)

P(1)-N(1)	1.587(6)	B(2)-B(3)	1.791(13)	B(7)-B(10)	1.648(15)	B(3')-H(3')	0.99(3)
P(1)-C(111)	1.796(4)	B(2)-B(5)	1.899(14)	B(7)-H(7)	1.27(3)	B(4')-B(5')	1.719(17)
P(1)-C(121)	1.792(4)	B(2)-B(6)	1.948(14)	B(8)-B(10)	1.810(16)	B(4')-B(7')	1.760(16)
P(1)-C(131)	1.789(4)	B(2)-H(2)	1.19(3)	B(8)-H(8)	1.09(3)	B(4')-B(8')	1.705(17)
P(2)-N(1)	1.559(6)	B(2)-H(25)	1.27(3)	B(8)-H(810)	1.43(3)	B(4')-H(4')	1.14(3)
P(2)-C(211)	1.797(4)	B(3)-B(4)	1.765(13)	B(10)-H(10)	1.07(3)	B(5')-B(8')	1.802(17)
P(2)-C(221)	1.797(4)	B(3)-B(6)	1.781(14)	B(10)-H(610)	1.16(3)	B(5')-H(5')	1.38(3)
P(2)-C(231)	1.795(4)	B(3)-B(7)	1.814(13)	B(10)-H(810)	1.18(3)	B(5')-H(25')	1.40(3)
P(3)-N(2)	1.577(5)	B(3)-H(3)	1.18(3)	B(1')-B(2')	1.670(20)	B(6')-B(7')	1.745(17)
P(3)-C(311)	1.800(4)	B(4)-B(5)	1.747(14)	B(1')-B(3')	1.747(20)	B(6')-B(10')	1.768(17)
P(3)-C(321)	1.793(4)	B(4)-B(7)	1.812(13)	B(1')-B(4')	1.680(19)	B(6')-H(6')	1.10(3)
P(3)-C(331)	1.789(4)	B(4)-B(8)	1.761(14)	B(1')-B(5')	1.567(20)	B(6')-H(610')	1.28(3)
P(4)-N(2)	1.565(5)	B(4)-H(4)	1.21(3)	B(1')-H(1')	1.65(4)	B(7')-B(8')	1.839(17)
P(4)-C(411)	1.785(4)	B(5)-B(8)	1.891(15)	B(2')-B(3')	1.760(17)	B(7')-B(10')	1.596(16)
P(4)-C(421)	1.796(4)	B(5)-H(5)	1.22(3)	B(2')-B(5')	1.936(18)	B(7')-H(7')	0.81(3)
P(4)-C(431)	1.794(4)	B(5)-H(25)	1.18(3)	B(2')-B(6')	1.869(18)	B(8')-B(10')	1.741(17)
B(1)-B(2)	1.700(13)	B(6)-B(7)	1.788(14)	B(2')-H(2')	1.05(3)	B(8')-H(8')	0.91(3)
B(1)-B(3)	1.682(13)	B(6)-B(10)	1.797(16)	B(2')-H(25')	1.59(3)	B(8')-H(810')	1.23(3)
B(1)-B(4)	1.656(13)	B(6)-H(6)	1.27(3)	B(3')-B(4')	1.763(16)	B(10')-H(10')	0.92(3)
B(1)-B(5)	1.669(14)	B(6)-H(610)	1.51(3)	B(3')-B(6')	1.685(17)	B(10')-H(610')	1.43(3)
B(1)-H(1)	0.98(3)	B(7)-B(8)	1.807(14)	B(3')-B(7')	1.740(17)	B(10')-H(810')	1.29(3)

Table 5. Interbond angles (°) for (1)

N(1)-P(1)-C(111)	109.69(24)	B(3')-B(2')-B(5')	86.8(8)	B(2)-B(6)-B(7)	99.8(6)	B(6)-B(7)-B(8)	101.7(7)
N(1)-P(1)-C(121)	110.01(24)	B(3')-B(2')-B(6')	55.2(7)	B(2)-B(6)-B(10)	108.9(7)	B(6)-B(7)-B(10)	62.9(6)
N(1)-P(1)-C(131)	114.27(24)	B(3')-B(2')-H(2')	152.7(21)	B(1')-B(4')-B(3')	60.9(8)	B(6)-B(7)-H(7)	118.3(16)
C(111)-P(1)-C(121)	106.59(17)	B(5')-B(2')-B(6')	103.3(8)	B(1')-B(4')-B(5')	54.9(8)	B(8)-B(7)-B(10)	63.0(6)
C(111)-P(1)-C(131)	107.82(17)	B(5')-B(2')-H(2')	118.0(20)	B(1')-B(4')-B(7')	115.6(9)	B(8)-B(7)-H(7)	133.0(16)
C(121)-P(1)-C(131)	108.16(17)	B(6')-B(2')-H(2')	122.7(20)	B(1')-B(4')-B(8')	114.2(9)	B(10)-B(7)-H(7)	113.5(16)
N(1)-P(2)-C(211)	108.80(24)	B(1')-B(2')-H(25')	96.2(14)	B(1')-B(4')-H(4')	119.0(19)	B(4)-B(8)-B(5)	57.0(5)
N(1)-P(2)-C(221)	110.44(24)	B(3')-B(2')-H(25')	109.9(14)	B(3')-B(4')-B(5')	93.8(8)	B(4)-B(8)-B(7)	61.0(5)
N(1)-P(2)-C(231)	116.48(25)	B(5')-B(2')-H(25')	45.4(12)	B(3')-B(4')-B(7')	59.2(7)	B(4)-B(8)-B(10)	109.4(7)
C(211)-P(2)-C(221)	106.83(17)	H(2')-B(2')-H(25')	96.5(23)	B(3')-B(4')-B(8')	105.7(8)	B(4)-B(8)-H(8)	120.2(19)
C(211)-P(1)-C(231)	107.05(18)	B(1')-B(3')-B(2')	56.9(8)	B(3')-B(4')-H(4')	121.1(18)	B(4)-B(8)-H(810)	132.0(15)
C(221)-P(2)-C(231)	106.80(18)	B(1')-B(3')-B(4')	57.2(7)	B(5')-B(4')-B(7')	108.6(8)	B(5)-B(8)-B(7)	98.9(7)
P(1)-N(1)-P(2)	144.7(4)	B(1')-B(3')-B(6')	117.8(10)	B(5')-B(4')-B(8')	63.5(7)	B(5)-B(8)-B(10)	108.1(7)
N(2)-P(3)-C(311)	109.14(24)	B(1')-B(3')-B(7')	113.3(9)	B(5')-B(4')-H(4')	137.2(19)	B(5)-B(8)-H(8)	129.4(19)
N(2)-P(3)-C(321)	109.29(24)	B(1')-B(3')-H(3')	121.9(21)	B(7')-B(4')-B(8')	64.1(7)	B(5)-B(8)-H(810)	92.9(14)
N(2)-P(3)-C(331)	113.94(24)	B(2')-B(3')-B(4')	91.9(8)	B(7')-B(4')-H(4')	110.4(18)	B(7)-B(8)-B(10)	54.2(6)
C(311)-P(3)-C(321)	107.90(17)	B(2')-B(3')-B(6')	65.7(7)	B(8')-B(4')-H(4')	121.0(18)	B(7)-B(8)-H(8)	124.7(19)
C(311)-P(3)-C(331)	108.22(17)	B(2')-B(3')-B(7')	106.0(8)	B(1')-B(5')-B(2')	55.8(8)	B(7)-B(8)-H(810)	92.9(14)
C(321)-P(3)-C(331)	108.19(17)	B(2')-B(3')-H(3')	123.4(21)	B(1')-B(5')-B(4')	61.3(8)	B(10)-B(8)-H(8)	117.6(19)
N(2)-P(4)-C(411)	110.05(24)	B(4')-B(3')-B(6')	106.1(8)	B(1')-B(5')-B(8')	114.9(10)	B(10)-B(8)-H(810)	40.4(14)
N(2)-P(4)-C(421)	115.33(24)	B(4')-B(3')-B(7')	60.3(7)	B(1')-B(5')-H(5')	119.9(17)	H(8)-B(8)-H(810)	107.7(22)
N(2)-P(4)-C(431)	108.96(24)	B(4')-B(3')-H(3')	138.7(21)	B(1')-B(5')-H(25')	109.9(16)	B(6)-B(10)-B(7)	62.4(6)
C(411)-P(4)-C(421)	106.29(18)	B(6')-B(3')-B(7')	61.2(7)	B(2')-B(5')-B(4')	87.5(8)	B(6)-B(10)-B(8)	101.3(7)
C(411)-P(4)-C(431)	107.22(17)	B(6')-B(3')-H(3')	107.9(21)	B(2')-B(5')-B(8')	100.2(8)	B(6)-B(10)-H(10)	122.3(19)
C(421)-P(4)-C(431)	108.67(18)	B(7')-B(3')-H(3')	119.4(21)	B(2')-B(5')-H(5')	140.7(16)	B(6)-B(10)-H(610)	56.6(17)
P(3)-N(2)-P(4)	146.5(4)	B(6)-B(2)-H(25)	90.7(16)	B(2')-B(5')-H(25')	54.2(14)	B(6)-B(10)-H(810)	112.4(18)
B(2)-B(1)-B(3)	63.9(6)	H(2)-B(2)-H(25)	108.6(22)	B(4')-B(5')-B(8')	57.9(7)	B(4')-B(7')-B(6')	103.7(8)
B(2)-B(1)-B(4)	99.4(7)	B(1)-B(3)-B(2)	58.5(5)	B(4')-B(5')-H(5')	126.9(16)	B(4')-B(7')-B(8')	56.5(6)
B(2)-B(1)-B(5)	68.6(6)	B(1)-B(3)-B(4)	57.4(5)	B(4')-B(5')-H(25')	112.6(16)	B(4')-B(7')-B(10')	112.9(9)
B(2)-B(1)-H(1)	130.1(20)	B(1)-B(3)-B(6)	119.9(7)	B(8')-B(5')-H(5')	113.7(16)	B(4')-B(7')-H(7')	112.2(25)
B(3)-B(1)-B(4)	63.8(6)	B(1)-B(3)-B(7)	114.1(7)	B(8')-B(5')-H(25')	75.6(15)	B(6')-B(7')-B(8')	97.3(8)
B(3)-B(1)-B(5)	98.1(7)	B(1)-B(3)-H(3)	126.5(17)	H(5')-B(5')-H(25')	114.7(20)	B(6')-B(7')-B(10')	63.7(7)
B(3)-B(1)-H(1)	134.9(20)	B(2)-B(3)-B(4)	92.1(6)	B(2')-B(6')-B(3')	59.1(7)	B(6')-B(7')-H(7')	142.4(26)
B(4)-B(1)-B(5)	63.4(6)	B(2)-B(3)-B(6)	66.1(6)	B(2')-B(6')-B(7')	101.3(8)	B(8')-B(7')-B(10')	60.4(7)
B(4)-B(1)-H(1)	130.5(20)	B(2)-B(3)-B(7)	104.9(6)	B(2')-B(6')-B(10')	109.2(8)	B(8')-B(7')-H(7')	111.5(25)
B(5)-B(1)-H(1)	126.9(20)	B(2)-B(3)-H(3)	132.9(17)	B(2')-B(6')-H(6')	122.8(19)	B(10')-B(7')-H(7')	109.7(25)
B(1)-B(2)-B(3)	57.5(5)	B(4)-B(3)-B(6)	106.1(6)	B(2')-B(6')-H(610')	90.1(16)	B(4')-B(8')-B(5')	58.6(7)
B(1)-B(2)-B(5)	54.9(5)	B(4)-B(3)-B(7)	60.8(5)	B(3')-B(6')-B(7')	60.9(7)	B(4')-B(8')-B(7')	59.4(7)
B(1)-B(2)-B(6)	110.4(7)	B(4)-B(3)-H(3)	132.1(17)	B(3')-B(6')-B(10')	109.2(9)	B(4')-B(8')-B(10')	108.5(8)
B(1)-B(2)-H(2)	125.1(17)	B(6)-B(3)-B(7)	59.7(5)	B(3')-B(6')-H(6')	115.7(19)	B(4')-B(8')-H(8')	126.6(23)
B(1)-B(2)-H(25)	92.2(16)	B(6)-B(3)-H(3)	107.2(17)	B(3')-B(6')-H(610')	139.4(17)	B(4')-B(8')-H(810')	128.8(18)
B(3)-B(2)-B(5)	86.6(6)	B(7)-B(3)-H(3)	110.5(17)	B(7')-B(6')-B(10')	54.0(7)	B(5')-B(8')-B(7')	101.8(8)
B(3)-B(2)-B(6)	56.7(5)	B(1)-B(4)-B(3)	58.8(5)	B(7')-B(6')-H(6')	126.5(19)	B(5')-B(8')-B(10')	115.8(9)
B(3)-B(2)-H(2)	140.7(17)	B(1)-B(4)-B(5)	58.7(5)	B(7')-B(6')-H(610')	106.0(17)	B(5')-B(8')-H(8')	115.0(23)
B(3)-B(2)-H(25)	110.5(16)	B(1)-B(4)-B(8)	120.5(7)	B(10')-B(6')-H(6')	123.3(19)	B(5')-B(8')-H(810')	89.1(17)
B(5)-B(2)-B(6)	101.3(6)	B(1)-B(4)-H(4)	115.7(17)	B(10')-B(6')-H(610')	53.2(15)	B(7')-B(8')-B(10')	52.9(6)
B(5)-B(2)-H(2)	129.0(17)			H(6')-B(6')-H(610')	102.9(24)	B(7')-B(8')-H(8')	139.1(23)

Table 5 *(continued)*

B(5)-B(2)-H(25)	37.3(15)	B(3)-B(4)-B(5)	92.3(6)	B(3')-B(7')-B(4')	60.5(7)	B(7')-B(8')-H(810')	95.5(17)
B(6)-B(2)-H(2)	119.2(17)	B(3)-B(4)-B(7)	60.9(5)	B(3')-B(7')-B(6')	57.9(7)	B(10')-B(8')-H(8')	118.5(23)
B(7)-B(10)-B(8)	62.8(6)	B(3)-B(4)-B(8)	107.5(7)	B(3')-B(7')-B(8')	101.1(8)	B(10')-B(8')-H(810')	47.9(16)
B(7)-B(10)-H(10)	125.1(20)	B(3)-B(4)-H(4)	133.1(17)	B(3')-B(7')-B(10')	115.1(9)	H(8')-B(8')-H(810')	102.0(27)
B(7)-B(10)-H(610)	112.1(18)	B(5)-B(4)-B(7)	104.3(6)	B(3')-B(7')-H(7')	133.5(25)	B(6')-B(10')-B(7')	62.2(7)
B(7)-B(10)-H(810)	112.4(18)	B(5)-B(4)-B(8)	65.2(6)	B(2)-B(6)-H(6)	122.2(16)	B(6')-B(10')-B(8')	100.2(8)
B(8)-B(10)-H(10)	134.6(20)	B(5)-B(4)-H(4)	126.4(17)	B(3)-B(6)-B(7)	61.1(5)	B(6')-B(10')-H(10')	147.5(23)
B(8)-B(10)-H(610)	102.4(18)	B(7)-B(4)-B(8)	60.8(5)	B(3)-B(6)-B(10)	109.9(7)	B(6')-B(10')-H(610')	45.8(14)
B(8)-B(10)-H(810)	52.1(16)	B(7)-B(4)-H(4)	121.1(17)	B(3)-B(6)-H(6)	117.0(16)	B(6')-B(10')-H(810')	100.2(16)
H(10)-B(10)-H(610)	111.3(25)	B(8)-B(4)-H(4)	112.3(17)	B(7)-B(6)-B(10)	54.7(6)	B(7')-B(10')-B(8')	66.7(7)
H(10)-B(10)-H(810)	113.1(25)	B(1)-B(5)-B(2)	56.5(5)	B(7)-B(6)-H(6)	128.9(16)	B(7')-B(10')-H(10')	133.8(23)
H(610)-B(10)-H(810)	69.8(23)	B(1)-B(5)-B(4)	58.0(5)	B(10)-B(6)-H(6)	123.4(16)	B(7')-B(10')-H(610')	106.7(15)
B(2')-B(1')-B(3')	61.9(8)	B(1)-B(5)-B(8)	112.8(7)	B(2)-B(6)-H(610)	86.7(13)	B(7')-B(10')-H(810')	105.6(16)
B(2')-B(1')-B(4')	98.1(10)	B(1)-B(5)-H(5)	123.6(17)	B(3)-B(6)-H(610)	124.7(14)	B(8')-B(10')-H(10')	112.1(22)
B(2')-B(1')-B(5')	73.4(9)	B(1)-B(5)-H(25)	97.3(17)	B(7)-B(6)-H(610)	90.3(13)	B(8')-B(10')-H(610')	110.3(15)
B(3')-B(1')-B(4')	61.9(8)	B(2)-B(5)-B(4)	89.1(6)	B(10)-B(6)-H(610)	40.0(13)	B(8')-B(10')-H(810')	44.9(15)
B(3')-B(1')-B(5')	100.1(10)	B(2)-B(5)-B(8)	105.5(7)	H(6)-B(6)-H(610)	117.6(20)	H(10')-B(10')-H(610')	115.5(26)
B(4')-B(1')-B(5')	63.8(8)	B(2)-B(5)-H(5)	121.2(17)	B(3)-B(7)-B(4)	58.3(5)	H(10')-B(10')-H(810')	100.4(26)
B(2')-B(1')-H(1')	128.3(15)	B(2)-B(5)-H(25)	40.9(16)	B(3)-B(7)-B(6)	59.2(5)	H(610')-B(10')-H(810')	78.6(20)
B(3')-B(1')-H(1')	125.2(15)	B(4)-B(5)-B(8)	57.8(5)	B(3)-B(7)-B(8)	103.5(6)	B(2)-H(25)-B(5)	101.8(24)
B(4')-B(1')-H(1')	131.9(15)	B(4)-B(5)-H(5)	145.9(17)	B(3)-B(7)-B(10)	115.4(7)	B(6)-H(610)-B(10)	83.4(20)
B(5')-B(1')-H(1')	134.6(16)	B(4)-B(5)-H(25)	115.1(17)	B(3)-B(7)-H(7)	117.2(16)	B(2')-H(25')-B(5')	80.4(17)
B(1')-B(2')-B(3')	61.2(8)	B(8)-B(5)-H(5)	119.9(17)	B(4)-B(7)-B(6)	103.8(6)	B(8)-H(810)-B(10)	87.5(21)
B(1')-B(2')-B(5')	50.9(7)	B(8)-B(5)-H(25)	92.7(17)	B(4)-B(7)-B(8)	58.2(5)	B(6')-H(610')-B(10')	81.0(19)
B(1')-B(2')-B(6')	112.1(10)	H(5)-B(5)-H(25)	98.8(23)	B(4)-B(7)-B(10)	114.7(7)	B(8')-H(810')-B(10')	87.3(21)
B(1')-B(2')-H(2')	124.5(21)	B(2)-B(6)-B(3)	57.2(5)	B(4)-B(7)-H(7)	126.3(16)		

observed. Separation of the bulk material by chromatography on silica (eluant CH$_2$Cl$_2$) resulted in the isolation of the second component, whose ^{11}B n.m.r. spectrum was identical to that of B$_9$H$_{13}$(NCMe).[24] Subsequent experiments with the addition of supporting electrolyte to the anolyte gave similar products.

Anodic Dissolution of Metals in Solutions of [B$_9$H$_{12}$]$^-$.— Solutions of [NMe$_4$][B$_9$H$_{12}$] (0.1 mol dm^{-3}) or [N(PPh$_3$)$_2$][B$_9$H$_{12}$] (6.8 × 10^{-3} mol dm^{-3}) in MeCN were prepared and cyclic voltammograms obtained, using the metal under study as the working electrode, Pt wire as the secondary electrode, and Ag–AgNO$_3$ (0.1 mol dm^{-3}) as reference. Extrapolation of the essentially linear portion of the voltammogram to zero current gave the effective dissolution potential for the metals which underwent anodic dissolution in the solution, or the effective potential of anion oxidation for metals which did not dissolve.
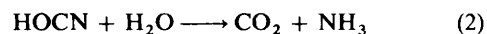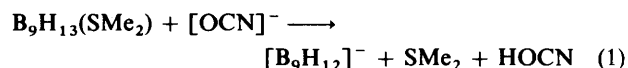
*Stereospecific Preparation of anti-*B$_{18}$H$_{22}$.—A solution of [NBu$^n_4$][B$_9$H$_{12}$] (2.16 g, 6.14 mmol) was prepared by condensing dry, degassed CH$_2$Cl$_2$ (30 cm^3) onto the solid contained in an evacuated flask, and warming to room temperature until the solid had dissolved. The solution was cooled to −196 °C, gaseous HCl (0.37 g, 10 mmol) was condensed in, and the mixture warmed to room temperature. After the initial mild gas evolution, the solution was stirred for 3 h and the solvent removed under reduced pressure to give an oil which crystallised overnight. T.l.c. analysis showed a single major product (R_f = 0.8 using CH$_2$Cl$_2$ eluant) and the product was purified by column chromatography to give a pale yellow solid (yield 0.86 g, 65%), identified as *anti-*B$_{18}$H$_{22}$ by comparison of its ^{11}B n.m.r. spectrum with that of an authentic sample.

Preparation of anti-[B$_{18}$H$_{21}$]$^-$.—To a solution of [NBu$^n_4$][B$_9$H$_{12}$] (3 mmol) in CH$_2$Cl$_2$ (30 cm^3), prepared under vacuum, was added an excess of CF$_3$CO$_2$H dropwise, and the mixture stirred for 1 h. The addition resulted in immediate gas evolution, and the colourless solution became pale yellow. T.l.c. analysis (CH$_2$Cl$_2$ eluant) indicated a major product (R_f = 0.48) and a minor component (R_f = 0.77). After separation by

column chromatography on silica, the minor component was identified as B$_{10}$H$_{14}$ by comparison of its ^{11}B n.m.r. spectrum with an authentic sample. The major component, obtained in good yield (60%) was identified from its ^{11}B and ^{1}H-{^{11}B, c.w.} n.m.r. spectra (Table 2) as *anti-*[B$_{18}$H$_{21}$]$^-$.

Results and Discussion

(a) *Preparations.*—The [B$_9$H$_{12}$]$^-$ anion has been prepared cleanly as a [N(PPh$_3$)$_2$]$^+$ salt from the reaction between B$_9$H$_{13}$(SMe$_2$) and [N(PPh$_3$)$_2$][OCN]; the by-products were volatile (SMe$_2$) or gave volatile hydrolysis products on work-up [equations (1) and (2)]. The [OCN]$^-$ anion acted as a

$$B_9H_{13}(SMe_2) + [OCN]^- \longrightarrow$$
$$[B_9H_{12}]^- + SMe_2 + HOCN \quad (1)$$

$$HOCN + H_2O \longrightarrow CO_2 + NH_3 \quad (2)$$

deprotonating base. Deprotonation was also obtained with the bases LiN(CH$_2$Ph)$_2$ or LiN=C(NMe$_2$)$_2$, although the reactions were less clean and a more tedious work-up procedure was necessary to give a product of good purity. Furthermore, in the case of reactions of LiN=C(NMe$_2$)$_2$ with B$_9$H$_{13}$(SMe$_2$), the major product was the neutral species B$_9$H$_{13}$[HN=C(NMe$_2$)$_2$]. The ^{11}B and ^{1}H n.m.r. spectra (Table 1) of this by-product indicated that it was the first fluxional neutral B$_9$H$_{13}$L derivative.[24]

(b) X-*Ray Crystal and Molecular Structure of* (1).—Table 3 lists the final positional parameters of the refined atoms.* In Table 4 are listed the bond distances and in Table 5 the interbond angles derived.

There are two crystallographically independent ion pairs in the asymmetric fraction of the unit cell. Within experimental error, the two [B$_9$H$_{12}$]$^-$ ions are superimposable {as are the

---

* Atomic numbering scheme: C(*ij*1)—C(*ij*6) are phenyl carbons numbered cyclically, with C(1*jl*) (*j* = 1—3) bound to P(1), C(2*jl*) (*j* = 1—3) bound to P(2), *etc.*
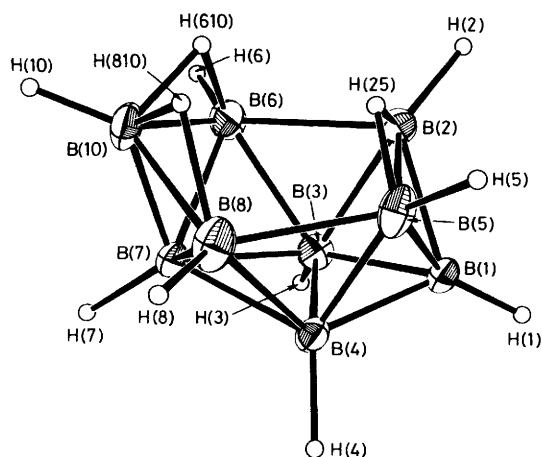
Figure 1. Perspective view of the $[B_9H_{12}]^-$ anion, with the thermal ellipsoids of boron drawn at the 30% probability level. The hydrogen atoms have an artificial radius of 0.1 Å for clarity

$[N(PPh_3)_2]^+$ cations} and a perspective view of one anion is presented in Figure 1, which also demonstrates the atomic numbering system.[25] The second anion is numbered similarly and is identified by primes.

The overall architecture of the anion is that of a *nido*-nine-vertex cage, a geometrical fragment of a bicapped square antiprism with one 5-connected† vertex removed. The pentagonal open face thus created is symmetrically bridged by three μ-hydrogen atoms, affording the cage effective C_s symmetry. Thus, there are 11 skeletal electron pairs available for cluster bonding and, hence, the polyhedral geometry is that predicted by empirical electron-counting procedures.[26]

In the present study, all hydrogen atoms associated with the borane polyhedra have been successfully located and positionally refined.

All three bridging hydrogen atoms in the $[B_9H_{12}]^-$ anion are disposed inward towards a position above the pentagonal open face, and thus lie more within the polyhedral surface than outside it. With respect to their edge-fused B_3 triangles, the B(6)B(10)H(610) and B(8)B(10)H(810) triangles bend inward, by *ca.* 32 and 20°, respectively for the unprimed molecule and by 15 and 32° respectively for the primed molecule. These angles are complemented by short apparent H $\cdots$ H distances of 1.34(5) and 1.73(5) Å for unprimed and primed molecules respectively. Given the relative inaccuracy of the hydrogen-atom co-ordinates in the present study, it is clearly inappropriate to attempt to interpret these asymmetries; by comparison, a very accurate determination[27] of $B_{10}H_{14}$ affords bend-in angles of 21.0 and 21.8° and an H $\cdots$ H contact of 1.944 Å.

In contrast, the third bridging atom, H(25), lies within 3° of the plane of the appropriate edge-fused B_3 triangle $[B(1)B(2)B(5)]$ in both crystallographically independent anions. For this part of the $[B_9H_{12}]^-$ polyhedron, the most relevant reference compound against which to compare this feature is B_5H_9. Structural studies by *X*-ray diffraction, electron diffraction, and microwave spectroscopy agree that the bridging hydrogens in B_5H_9 are bent towards the open square face by between 7 and 16°.[10b] In $[B_9H_{12}]^-$ the apparent distances between the two types of bridging hydrogens lie within the range 1.45(5)—2.09(5) Å.

In the crystal structure of (1) there are no close contacts between ions. The two crystallographically independent $[N(PPh_3)_2]^+$ cations are bent at nitrogen [144.7(4)° for

† Connectivity numbers are expressed only with respect to the polyhedron.

$P(1)-N(1)-P(2)$, 146.5(4)° for $P(3)-N(2)-P(4)$] and adopt an eclipsed conformation about their $P \cdots P$ vectors with a 'mean torsion angle'[28] of 5.8(3) and 4.3(3)°, respectively. Each cation also possesses a strong intramolecular quasi-graphitic interaction, between rings 23 and 13 $[P(1)-N(1)-P(2)$, centroid–centroid distance 3.695(5) Å, dihedral angle 5.4(3)°] and between rings 33 and 42 $[P(3)-N(2)-P(4)$, 3.713 Å, 10.3(3)°], where ring *ij* comprises $C(ij1)$—$C(ij6)$ and a centroid–centroid separation <4.7 Å is considered significant.[29]

A diagram of the contents of one unit cell viewed approximately along the *b* axis towards the origin has been deposited in SUP 56224.

(c) *N.M.R. Spectra.*—The ^{11}B and $^{11}B-\{^1H\}$ spectra (Figure 2) of the $[B_9H_{12}]^-$ anion have not been interpreted previously, partly as a result of the unknown structure of the anion and partly as a result of the inadequate understanding of the variations of ^{11}B chemical shifts with cage structure. Two-dimensional (2D) $^{11}B-^{11}B$ (COSY) n.m.r. has been shown recently[30,31] to be of substantial help in both the assignment of the spectra of boron cages of known structure and also in deducing the structures of unknown compounds. The existence of $^{11}B-^{11}B$ couplings in the homonuclear 2D spectra has been established through the observation of cross peaks, and this has been shown to be significant only for boron atoms adjacent in the boron cluster. Coupling between boron atoms linked by bridging hydrogen atoms is usually absent. The 2D $^{11}B-^{11}B$ (COSY) n.m.r. spectrum of $[B_9H_{12}]^-$ is presented in Figure 3. Correlations between the chemical shifts of the ^1H resonances and the ^{11}B environments to which the protons are coupled have been obtained by examining the $^1H-\{^{11}B$, broad band} and $^1H-\{^{11}B$, c.w.} spectra. We have been able to observe at room temperature terminal hydrogen environments in the intensity ratio of $1:2:2:1:2:1$ by successive single-frequency decoupling at the boron resonance frequencies corresponding to the chemical shifts of the boron environments from high frequency (low field) to low frequency (high field), as indicated in Table 6. Greenwood and co-workers[12] reported similar shifts for most of the ^1H resonances but failed to resolve fully all the environments. At room temperature, the three bridging hydrogens were fluxional and occurred as a single resonance, whereas at -78 °C, Greenwood[12] found that this resolved into two resonances. Of these, that of area 2 near δ -3.0 p.p.m. was associated with the boron resonances near δ -10 and -14 p.p.m., whereas that of area 1 at δ -7.2 p.p.m. was associated only with the boron resonance near δ -34 p.p.m.

These low-temperature decoupling experiments established that the unique bridging hydrogen (δ -7.2 p.p.m.) was coupled to the two boron atoms at δ -34.1 p.p.m. and therefore identified these boron positions as $B(2,5)$ in Figure 1. Since some selective decoupling of the two bridging hydrogens (δ -3.0 p.p.m.) occurred by irradiation at $v(^{11}B)$ corresponding to δ -9.85 and either (or both) of δ -13.9, -14.5, the implication was one of two possibilities. Either (*i*) the resonance at δ -13.9 p.p.m. corresponded to $B(6,8)$ and one of the three resonances at δ -9.85 p.p.m. corresponded to $B(10)$; or (*ii*) two of the resonances at δ -9.85 corresponded to $B(6,8)$ and the resonance at δ -14.5 p.p.m. resulted from $B(10)$. In (*i*), the remaining two resonances at δ -9.85 must have been associated with $B(3,4)$; in (*ii*), the resonances at δ -13.9 p.p.m. must have resulted from $B(3,4)$. The ambiguity has been resolved by the couplings revealed by the 2D $^{11}B-^{11}B$ (COSY) data. Well pronounced coupling was observed between $B(2,5)$ at δ -34.1 p.p.m. and the resonances at δ -9.85 and -13.9 p.p.m., and this corresponded to the directly-bonded coupling of $B(2,5)$ to both $B(6,8)$ and $B(3,4)$. Similarly, the resonance at δ -13.9 p.p.m. showed coupling with δ -9.85 p.p.m. and $B(2,5)$ at δ -34.1 p.p.m., thus confirming that δ -13.9 and δ -9.85 p.p.m. arose
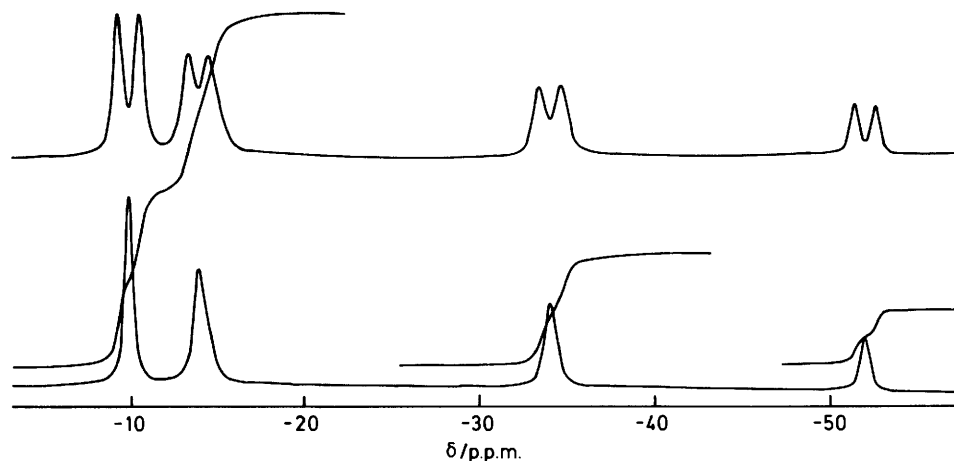
Figure 2. 115.5-MHz ^{11}B and ^{11}B-$\{^1$H, broad band$\}$ n.m.r. spectra of the $[B_9H_{12}]^-$ anion
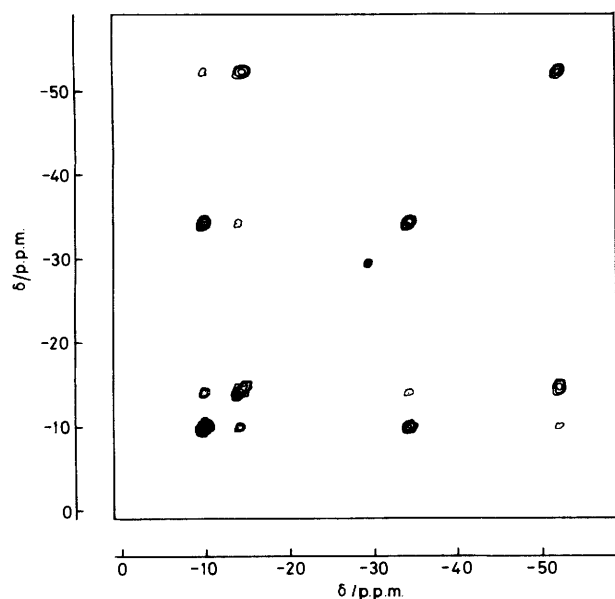
Figure 3. 2D ^{11}B–^{11}B (COSY) n.m.r. spectra of $[B_9H_{12}]^-$

Table 6. Correlations between boron-atom positions and ^{11}B and ^{1}H parameters for $[B_9H_{12}]^-$

Position	1	6,8	3,4	10	2,5	7
$\delta(^{11}$B)/p.p.m.	-9.85		-13.9	-14.5	-34.1	-51.9
Relative area	3		2	1	2	1
$\delta(^1$H)/p.p.m. (terminal)	2.75	1.68	1.74	2.58	0.72	-0.92
Relative area	1	2	2	1	2	1
$\delta(^1$H)/p.p.m. (bridge)		-3.0			-7.2	
Relative area		2			1	
^{11}B–^{11}B	A	B			B	B
Couplings	B	A			B	
(A with B)			A			B
	B	B			A	
	B			B		A

(d) Electrochemistry.—Voltammetry and coulometry. The electrochemical properties of $[B_9H_{12}]^-$ were found to be mechanistically complex and to be dependent substantially on the conditions, in particular, the solvent used. The cyclic (d.c.) voltammogram (c.v.) and the cyclic a.c. voltammogram of

from boron positions B(3,4) and B(6,8), respectively. Further support for the assignment resulted from the coupling of the resonance at δ −9.85 p.p.m. [due to B(6,8) and B(1)] with δ −34.1 p.p.m. [due to B(2,5)], δ −13.9 p.p.m. [due to B(3,4)], and the resonance at δ −51.9 p.p.m. [therefore due to B(7)]. Additionally, the resonance at δ −14.5 p.p.m. shows coupling only to that at δ −51.9 p.p.m., whereas the latter also couples with B(6,8). The resonances at δ −14.5 and −51.9 p.p.m. are thus unambiguously established as borons B(10) and B(7), respectively. The details of the correlation between the boron atom positions and ^{11}B shifts, ^{1}H shifts, and ^{11}B–^{11}B couplings are summarised in Table 6.

The observed 2D ^{11}B–^{11}B (COSY) couplings are fully in accord with the stereochemical arrangement shown in Figure 1.

$[NBu^n_4][B_9H_{12}]$ in MeCN at Pt are presented in Figure 4. The oxidation wave in the c.v. near 1.4 V, whose degree of reversibility was uncertain, corresponded to a peak in the a.c. voltammogram near 1.1 V whose superimposition of forward and reverse scans suggested an electrochemical process which was close to being reversible.[32] In addition, the weak reduction wave near −0.8 V was not observed in scans which did not encompass the oxidation and, thus, must have arisen as a result of a reduction of a product of oxidation.

Constant potential coulometry at 0.86 V resulted in the consumption of one electron per mol of $[B_9H_{12}]^-$, and characterisation of the products in solution by n.m.r. showed that $B_9H_{13}(MeCN)$ was the only identifiable soluble product. Some insoluble material precipitated during the electrolysis and has not yet been characterised. The mass spectra of the solid products indicated a small quantity of $B_{18}H_{22}$. In order for a derivative containing more hydrogen than the original anion to have been produced, it is likely that a radical produced as a result of the electrochemical oxidation subsequently abstracted hydrogen from a compound in the vicinity of the radical. In an attempt to ascertain whether this radical reaction occurred with solvent, the electrolysis was carried out in CD_3CN and the products monitored by both ^{11}B n.m.r. and mass spectrometry. No evidence was found for specific positional deuteriation of boron in the ^{11}B spectra of the electrochemically produced
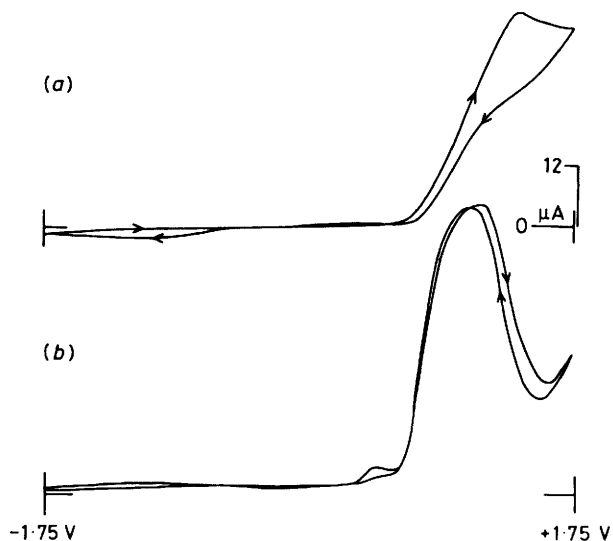
Figure 4. (a) Cyclic (d.c.) voltammogram (scan rate 30 V min^{-1}) and (b) a.c. voltammogram (scan rate 3 V min^{-1}; a.c. 100 Hz) of [N(PPh$_3$)$_2$][B$_9$H$_{12}$] at Pt in MeCN

B$_9$H$_{13}$(CD$_3$CN), and the mass spectra failed to reveal clearly that deuteriation had occurred at all, although ions due to B$_{18}$H$_{22}$ were observed. It was likely, therefore, that subsequent radical reactions took place either with other [B$_9$H$_{12}$]$^-$ ions or with the [N(PPh$_3$)$_2$]$^+$ cations.

When the voltammetry of [NBu$^n_4$][B$_9$H$_{12}$] was observed in the low-polarity solvents dichloromethane and 1,2-dichloroethane, the first oxidation wave was observed near 1.55 V. In the ether solvents tetrahydrofuran and 1,2-dioxolane, no clearly defined oxidation wave was observed below 1.6 V.

Coulometric oxidation of [NBu$^n_4$][B$_9$H$_{12}$] in CH$_2$Cl$_2$ at 1.2 V corresponded to less than a one-electron oxidation with the formation, primarily, of anti-[B$_{18}$H$_{21}$]$^-$. Chromatographic analysis indicated that the only significant by-product was a trace of B$_{10}$H$_{14}$.

A related isomer-specific oxidation of [B$_9$H$_{12}$]$^-$ to anti-[B$_{18}$H$_{21}$]$^-$ was recently reported by Greenwood and co-workers[33] through reaction of the nonaborate with [{Os(CO)$_3$-Cl$_2$}$_2$].

Anodic dissolution. The behaviour of metals as anodes in acetonitrile solutions of [B$_9$H$_{12}$]$^-$ may be characterised into three types, as has been observed previously for other borane anions.[34,35] Metals which underwent anodic dissolution, together with their effective dissolution potentials, were Zn (−0.78), Cd (−0.64), Cu (−0.40), Pb* (−0.25, 0.05), Ag (0.05), Co (0.05), and Al* (0.30, 0.76 V). Those which did not dissolve but enabled anion oxidation to occur, together with the effective oxidation potentials, were Au (0.58), Pd (0.67), Pt (0.70), Ni (0.70), Mo (0.75), and V (0.80 V). Metals which were essentially inert or passive, with low currents, together with their effective potentials, were W (0.85), Zr (0.86), Ti (1.25), Fe (1.29), Nb (1.33), and Ta (1.35 V).

(e) *Chemical Reactions.*—In previous work, [B$_9$H$_{12}$]$^-$ has been shown to react with HCl in ethers to give B$_9$H$_{13}$(OR$_2$) and in diethyl sulphide to give B$_9$H$_{13}$(SEt$_2$).[8,13] We have found that the reactions of protonic acids with [B$_9$H$_{12}$]$^-$ additionally depend both on the acid (e.g. HCl or CF$_3$CO$_2$H) and on the counter cation (e.g. [NBu$^n_4$]$^+$ or [N(PPh$_3$)$_2$]$^+$). Thus, the

reaction of HCl with [B$_9$H$_{12}$]$^-$ in the non-co-ordinating solvent CH$_2$Cl$_2$ resulted in addition to give [B$_9$H$_{13}$Cl]$^-$ when the cation was [N(PPh$_3$)$_2$]$^+$, but produced anti-B$_{18}$H$_{22}$ when the cation was [NBu$^n_4$]$^+$. The reaction of [NBu$^n_4$][B$_9$H$_{12}$] with CF$_3$CO$_2$H led instead to anti-[B$_{18}$H$_{21}$]$^-$, and this product presumably reflects the relative pK_a values of HCl, CF$_3$CO$_2$H, and B$_{18}$H$_{22}$. These reactions of [N(PPh$_3$)$_2$][B$_9$H$_{12}$] presumably proceed via protonation of a B–B bond, e.g., B(6)–B(2) [or B(8)–B(5)] to give the neutral intermediate B$_9$H$_{13}$. Attack of the ligand (OR$_2$, SR$_2$, or Cl$^-$) at B(2), with cleavage of the bridge B(6)–B(2) results in opening of the structure and conversion from the nido- to arachno-species. As a result of the fluxional nature of the bridge and potential endo-hydrogens, the observed products are B$_9$H$_{13}$L or [B$_9$H$_{13}$Cl]$^-$. The ^{11}B n.m.r. spectrum of [B$_9$H$_{13}$Cl]$^-$ is fully consistent with an anion which is fluxional at room temperature, as has been found previously for [B$_9$H$_{13}$(NCS)]$^-$ and related systems.[24] Reactions involving [NBu$^n_4$][B$_9$H$_{12}$] resulted in the intermediate B$_9$H$_{13}$ interacting with further [B$_9$H$_{12}$]$^-$ to form a B$_{18}$ derivative; this may reflect the formation of [NBu$^n_4$]Cl in which the Cl$^-$ ion is more extensively involved in ion-pair or ion-aggregate formation than in [N(PPh$_3$)$_2$]Cl.

Acknowledgements

References

1 B. M. Graybill, J. K. Ruff, and M. F. Hawthorne, *J. Am. Chem. Soc.*, 1961, **83**, 2669.

2 B. M. Graybill, A. R. Pitochelli, and M. F. Hawthorne, *Inorg. Chem.*, 1962, **1**, 626.

3 W. N. Lipscomb, 'Boron Hydrides,' W. A. Benjamin, New York, 1963, p. 187.

4 R. Rietz and R. Schaeffer, *J. Am. Chem. Soc.*, 1971, **93**, 1263.

5 J. C. Huffman and W. E. Streib, *J. Chem. Soc., Chem. Commun.*, 1972, 665.

6 R. Rietz and R. Schaeffer, *J. Am. Chem. Soc.*, 1973, **95**, 6524.

7 A. R. Siedle, G. M. Bodner, A. R. Garber, and L. J. Todd, *Inorg. Chem.*, 1974, **13**, 1756.

8 L. J. Todd and A. R. Siedle, *Prog. Nucl. Magn. Reson. Spectrosc.*, 1979, **13**, 87.

9 F. E. Wang, P. G. Simpson, and W. N. Lipscomb, *J. Am. Chem. Soc.*, 1961, **83**, 491.

10 (a) L. Barton, *Top. Curr. Chem.*, 1982, **100**, 169; (b) *ibid.*, p. 184.

11 R. D. Dobrott and W. N. Lipscomb, *J. Chem. Phys.*, 1962, **37**, 1779.

12 J. Bould, N. N. Greenwood, and J. D. Kennedy, *J. Chem. Soc., Dalton Trans.*, 1984, 2477.

13 (a) J. Dobson, P. G. Keller, and R. Schaeffer, *Inorg. Chem.*, 1968, **7**, 399; (b) D. F. Games, C. K. Nelson, and G. A. Steehler, *J. Am. Chem. Soc.*, 1984, **106**, 7266.

14 C. K. Nelson, *Diss. Abst. Int. B*, 1983, **43**, 2549.

15 W. Clegg, R. Snaith, H. M. M. Shearer, K. Wade, and G. Whitehead, *J. Chem. Soc., Dalton Trans.*, 1983, 1309.

16 D. Barr, W. Clegg, R. E. Mulvey, and R. Snaith, *J. Chem. Soc., Chem. Commun.*, 1984, 285.

17 P. Main, S. J. Fiske, S. E. Hull, L. Lessinger, G. Germain, J-P. Declercq, and M. M. Woolfson, MULTAN 80, A System of Computer Programs for the Automatic Solution of Crystal Structures from X-Ray Diffraction Data, Universities of York (England) and Louvain (Belgium), 1980.

18 G. M. Sheldrick, SHELX 76, A Program for Crystal Structure Determination, University of Cambridge, 1976.

19 P. Roberts and G. M. Sheldrick, XANADU, A Program for Crystallographic Calculations, University of Cambridge, 1976.

---

* Two potentials are quoted, since the anodic and cathodic scans were different, with the dissolution current higher on the cathodic scan.

20 J. M. Stewart, P. A. Machin, C. Dickinson, H. L. Ammon, H. Heck, and H. Flack, The XRAY 76 system, Technical Report TR-446, Computer Science Centre, University of Maryland, College Park, Maryland.
21 C. K. Johnson, ORTEP-II, Report ORNL-5138, Oak Ridge National Laboratory, Tennessee.
22 J. H. Morris and P. C. Choi, *J. Chem. Soc., Dalton Trans.*, 1984, 2119.
23 N. N. Greenwood and J. D. Kennedy, personal communication.
24 G. B. Jacobsen, J. H. Morris, and D. Reed, *J. Chem. Soc., Dalton Trans.*, 1984, 415.
25 J. B. Casey, W. J. Evans, and W. H. Powell, *Inorg. Chem.*, 1983, **22**, 2236.
26 K. Wade, *Chem. Commun.*, 1971, 792.
27 R. Brill, H. Dietrich, and H. Dierks, *Acta Crystallogr., Sect. B*, 1971, **27**, 2003.

28 C. Glidewell and D. C. Liles, *J. Organomet. Chem.*, 1981, **212**, 291.
29 A. J. Welch, Ph.D. Thesis, University of London, 1974.
30 D. Reed, *J. Chem. Res.*, 1984, (*S*) 198.
31 T. L. Venable, W. C. Hutton, and R. N. Grimes, *J. Am. Chem. Soc.*, 1984, **106**, 29.
32 A. J. Bard and L. R. Faulkner, 'Electrochemical Methods—Fundamentals and Applications,' John Wiley and Son, New York, 1980.
33 J. Bould, N. N. Greenwood, and J. D. Kennedy, *Polyhedron*, 1983, **2**, 1401.
34 J. H. Morris and D. Reed, *J. Chem. Res.*, 1980, (*S*) 282; (*M*) 3567.
35 G. B. Jacobsen, J. H. Morris, and D. Reed, *J. Chem. Res.*, 1982, (*S*) 319; (*M*) 3601.